Molecular modelling of the antiviral action of Resveratrol derivatives against the activity of two novel SARS CoV-2 and 2019-nCoV receptors

A. RANJBAR¹, M. JAMSHIDI¹, S. TORABI²

¹Nutrition Health Research Center, Hamadan University of Medical Sciences, Hamadan, Iran ²Department of Analytical Chemistry, Faculty of Chemistry, Bu-Ali Sina University, Hamadan, Iran

Abstract. The pandemic threat of COVID-19 causes serious concern for people and world organizations. The effect of Coronavirus disease on the lifestyle and economic status of humans is undeniable, and all of the researchers (biologists, pharmacists, physicians, and chemists) can help decrease its destructive effects. The molecular docking approach can provide a fast prediction of the positive influence the targets on the COVID-19 outbreak. In this work, we choose resveratrol (RV) derivatives (22 cases) and two newly released coordinate structures for COVID-19 as receptors [Papain-like Protease of SARS CoV-2 (PBD ID: 6W9C) and 2019-nCoV RNA-dependent RNA Polymerase (PBD ID: 6M71)]. The results show that conformational isomerism is significant and useful parameter for docking results. A wide spectrum of interactions such as Van der Waals, conventional hydrogen bond, Pi-donor hydrogen bond, Pi-Cation, Pi-sigma, Pi-Pi stacked, Amide-Pi stacked and Pi-Alkyl is detected via docking of RV derivatives and COVID-19 receptors. The potential inhibition effect of RV-13 (-184.99 kj/mol), and RV-12 (-173.76 kj/mol) is achieved at maximum value for 6W9C and 6M71, respectively.

Key Words:

SARS-CoV, COVID-19, Molecular docking, MolDock Score, Binding mode, Binding site.

Introduction

Coronavirus disease (COVID-19), a new pathogen, caused by Severe Acute Respiratory Syndrome Coronavirus (SARS-CoV) infection with an enhance in mortality and morbidity^{1,2}. The source or location of the COVID-19 outbreak was in Wuhan, China, and is impacting millions of humans with more than 60,000 deaths (https://www.worldometers.info/coronavirus/). Despite

extensive efforts by researchers to discover a drug or vaccine to reduce the destructive effects of the COVID-19, research laboratories or clinical trials have recently been conducting *in-vivo* and in-vitro trials to identify targets and their influence on preventing infection and COVID-19 progression²⁻⁵. World Health Organization (WHO) and other scientific institutes presented a variety of therapeutic targets that can influential and have potential inhibition against COVID-19^{6,7}. On January 25, 2020, Shanghai Institute of Materia Medica website, Chinese Academy of Sciences, reported thirty effective agents, such as polydatin, deoxyrhapontin, chalcone, (resveratrol derivatives), fosamprenavir, elvitegravir, tideglusib, carmofur, disulfiram, ebselen, shikonin, via treatment properties of COVID-197. Resveratrol's or trans-3,5,40-trihydroxy trans-stilbene derivatives are wide spectrums of polyphenol compounds with pharmacological features and multiple bio-functional activities, such as antiviral⁸⁻¹⁰, antiaging¹¹, anticancer¹², antidiabetic¹³, anticardiovascular¹⁴, antiobesity¹⁵, anti-oxidative stress (scavenging free radicals)16, antiproliferative¹⁷, and anti-Alzheimer's¹⁸. Resveratrol's can found in several plants, vegetables, beverages, and fruits extracts^{19,20}. Modern drug discovery can be achieved via applied intermolecular interactions of active compounds with targets (proteins)²¹. Molecular Docking, a high accuracy method, calculated the binding energy of different active modes of ligands in active sites of receptors and presented the best compound with suitable conformation for clinical trials²². A variety of softwares, such as Autodock 4.0, Autodock Vina, Molegro Virtual Docker, GOLD, FLEXX, and ZDOCK, have been represented for molecular modelling with several scoring functions and various algorithms [Incremental Construction (IC), Genetic Algorithm (GA), and Monte Carlo (MC)]^{23,24}. In this study, Molegro Virtual Docker (MVD) software²⁵ has carried out the docking of 23 ligands (Resveratrol derivatives) from ZINC database (https://zinc.docking.org/) and two recently COVID-19 receptors [Papain-like Protease of SARS CoV-2 (PBD ID: 6W9C) and 2019-nCoV RNA-dependent RNA Polymerase (PBD ID: 6M71)]. This approach can prepare a fast method for drug discovery or effective drugs to inhibition the activity of COVID-19. The RV-13 (ZINC code: ZINC100823228) and RV-12 (ZINC code: ZINC230079516) compound has the most therapeutic properties against 6W9C and 6M71, respectively, and the Coronavirus disease (COVID-19) outbreak (Figure 1).

Componential Protocol of COVID-19 Docking

In this work, Molegro Virtual Docker (MVD)²⁶ has been successfully performed for docking of useful RV derivatives (22 cases) with selected COVID-19 enzymes (2 cases) from PDB source (https://www.rcsb.org/) and calculated MolDock Score. The structure of RV derivatives was drawn using ChemBioDrawUltra and optimized *via*

MM2 force field procedures. Then, imported to MVD workspace in pdb format. The X-ray structure of enzymes is prepared with the elimination of water molecules and unique ligands via Discovery Studio 4.5 Client software. The cavities (binding sites) were identified automatically and chosen 30 cavities. MolDock SE is used as an algorithm in the docking wizard option. The MolDock scoring function was also set with a grid resolution of 0.30 A. The parameter setting was set at a maximum population size of 50, maximum iteration of 1,500 and, threshold energy of 100. Also, the simplex evolution section was set for 300 steps with a neighbor distance factor of 1.00. In Table I, the ZINC code, resveratrol (RV) derivative structures, and MolDock Score (kj/mol) have been reported.

Molecular Analysis of Resveratrol Derivatives with 6M71

Molecular docking simulation was carried out with MVD program and analyzed *via* Discovery Studio 4.5 Client software. For simplification, we only reported one of the high MolDock Score of resveratrol derivative (RV-12) with 6M71.

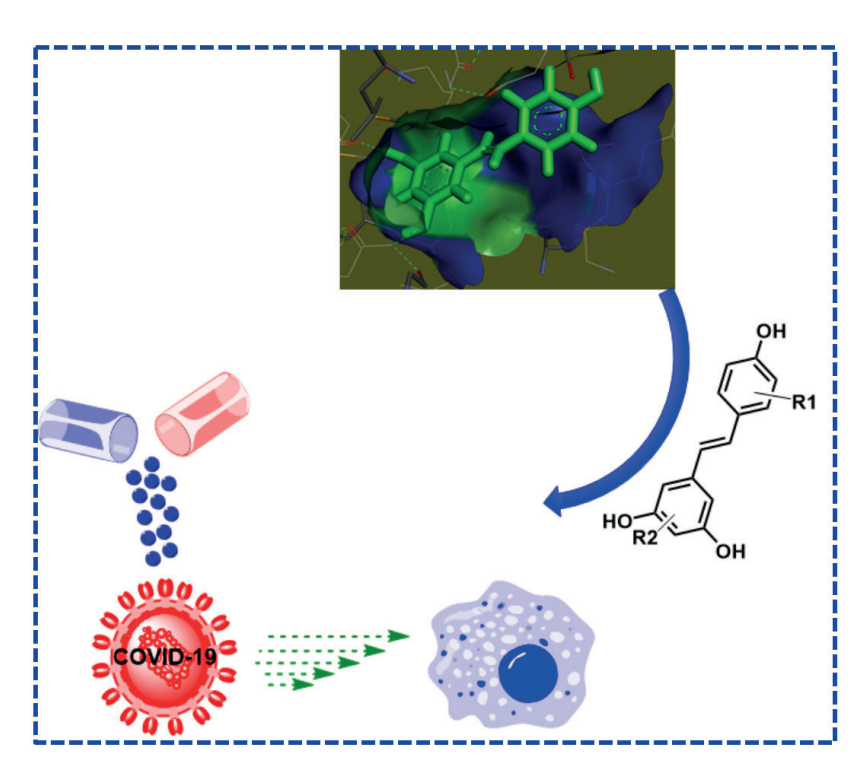


Figure 1. Molecular analysis of RV derivatives against COVID-19 receptors.

 $\textbf{Table I.} \ \ \text{The resveratrol (RV) derivative structures and their binding affinity (kj/mol) with two receptors (6M71 and 6W9C).}$

Compound name	RV derivative structures	MolDock Score (kj/mol)
RV-1 ZINC6787	НООН	6M71 (-93.59) 6W9C (-96.34)
RV-2 ZINC3978779	НО	6M71 (-97.14) 6W9C (-104.74)
RV-3 ZINC35653092	но	6M71 (-115.61) 6W9C (-116.63)
RV-4 ZINC4098633	OH HO,, OH OH	6M71 (-113.95) 6W9C (-133.20)
RV-5 ZINC15112536	HO OH OH	6M71 (-116.35) 6W9C (-130.93)
RV-6 ZINC40977346	НО	6M71 (-132.80) 6W9C (-138.28)
RV-7 ZINC15112538	но он он он он	6M71 (-113.35) 6W9C (-141.83)
RV-8 ZINC15112534	HO OH OH OH	6M71 (-118.18) 6W9C (-123.23)
RV-9 ZINC15112540	HO OH OH OH	6M71 (-114.79) 6W9C (-140.19)
RV-10 ZINC230079511	HO OH HO OH	6M71 (-172.47) 6W9C (-181.43)
RV-11 ZINC230079510	OH HO OH	6M71 (-164.20) 6W9C (-178.10)
	ÕН	Contin

Continued

 $\textbf{Table I (continued)}. \ \ \text{The resveratrol (RV) derivative structures and their binding affinity (kj/mol) with two receptors (6M71 and 6W9C)}.$

Compound name	RV derivative structures	MolDock Score (kj/mol)		
RV-12 ZINC230079516	HO OH HO OH	6M71 (-173.76) 6W9C (-177.56)		
RV-13 ZINC100823228	HO OH HO OH	6M71 (-145.93) 6W9C (-184.99)		
RV-14 ZINC85612047	OH HO OH HO OH	6M71 (-152.99) 6W9C (-165.25)		
RV-15 ZINC100823225	HO OH HO OH	6M71 (-154.18) 6W9C (-172.31)		
RV-16 ZINC230079516	HO OH OH OH	6M71 (-143.45) 6W9C (-171.70)		
RV-17 ZINC100827962	HO OH OH	6M71 (-156.86) 6W9C (-176.52)		
RV-18 ZINC100827965	OH OH OH	6M71 (-157.96) 6W9C (-171.45)		
RV-19 ZINC230097119	OH HO OH OH OH OH	6M71 (-159.17) 6W9C (-173.93)		
RV-20 ZINC230097112	OH HO OH	6M71 (-160.40) 6W9C (-162.54)		
RV-21 ZINC230097106	OH HO OH OH OH OH	6M71 (-144.37) 6W9C (-164.89)		
RV-22 ZINC230097101	OH OH OH	6M71 (-146.34) 6W9C (-161.80)		

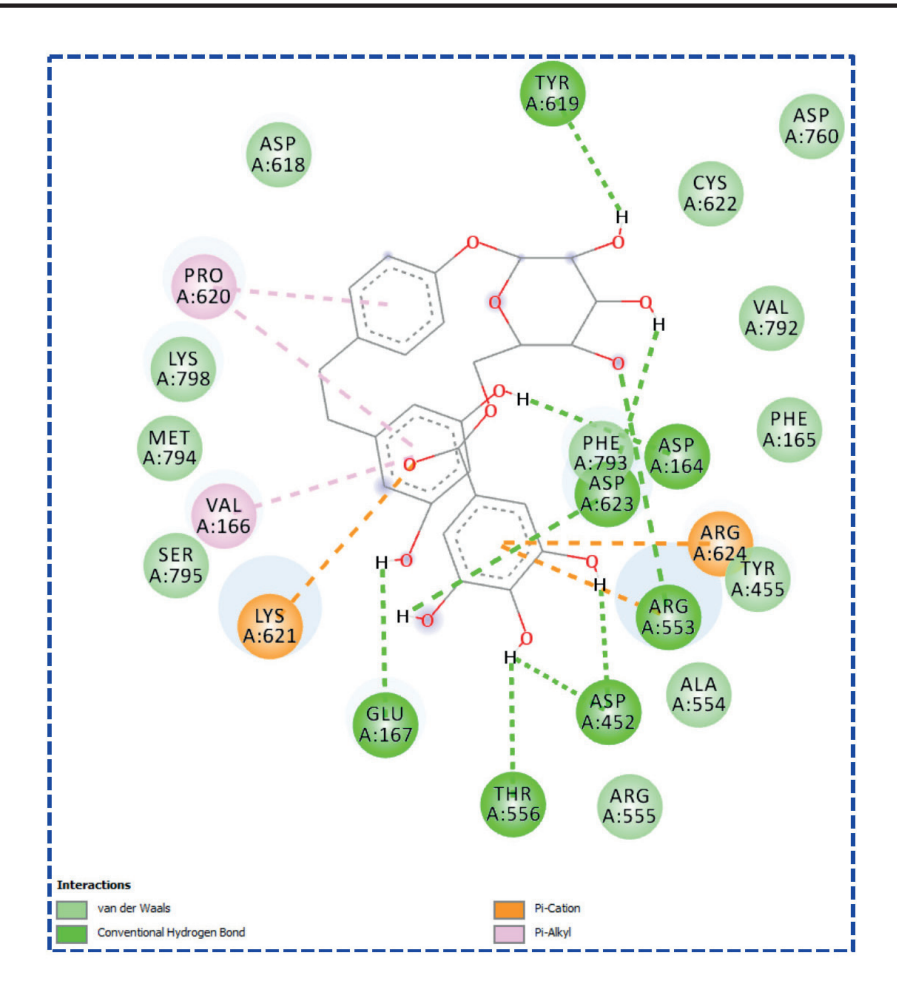


Figure 2. Binding residues and interactions of 6M71 with RV-12.

As shown in Figure 2, there are a variety types of interactions, such as Van der Waals, conventional hydrogen bond, Pi-Cation, and Pi-Alkyl between binding residues of 6M71 and different functional groups. Conventional hydrogen bonds are formed between GLU 167, THR 556, ASP 452, ARG 553, ASP 623, ASP 164, and TYR 619 with polar hydrogens and oxygen moiety. Interaction of Pi-orbitals and positive charge of ARG 553 and TYR 621 introduced electrostatic forces (Pi-cation). 1.3-Dihydroxy benzene and phenolic rings of RV-12 can interact with PRO 620 and VAL 166 and showed Pi-alkyl interaction. Also, the distance between two interaction factors (Angstrom) is given in Table II. The scoring results or interaction energies have been reported and, three best binding modes of RV are related to RV-12, 111, and 20. Conformational isomerism or conformer is one of the most effective parameters in molecular docking results²⁷. The binding orientations of structurally-related ligands in binding sites (cavities) can introduce a variety of interactions.

As shown in Table I, this phenomenon can be observed for docking results of RV-4 and RV-5, RV-11 and RV-12, RV-20 and RV-21. The binding affinity of conformers has differed for both receptors (6M71 and 6W9C).

In Cthe next step, the X-ray structure of 6M71 and the best conformation of ligand were overlaid in Discovery Studio 4.5 Client program, then showed ligand binding site atoms and created different surfaces around the ligand. Figure 3 (a-f) displayed receptor surfaces, such as aromatic edge/face, H-bond, charge, solvent accessibility surface (SAS)²⁸, hydrophobicity, and ionizability. The hydrophobicity surface indicated that the current receptor around the ligand has more hydrophilicity features (Figure 3a, blue color). The basic and acidic tendency of the receptor was indicated with the ionization surface, and their percentages are equal (Figure 3b, basic/blue color and acidic/red color). The solvent accessibility surface (SAS) or solvent-accessible surface area

Table II. The interaction results of RV-12 in binding site of 6M71.

Name	Distance	Category	Туре	From chemistry	To chemistry
A:ARG553:NH2 - P:POS1:O7	3.11346	Hydrogen Bond	Conventional Hydrogen Bond	H-Donor	H-Acceptor
P:POS1:H2 - A:ASP452:OD1	1.82777	Hydrogen Bond	Conventional Hydrogen Bond	H-Donor	H-Acceptor
P:POS1:H3 - A:ASP452:OD1	1.64674	Hydrogen Bond	Conventional Hydrogen Bond	H-Donor	H-Acceptor
P:POS1:H3 - A:THR556:OG1	2.66827	Hydrogen Bond	Conventional Hydrogen Bond	H-Donor	H-Acceptor
P:POS1:H4 - A:ASP623:OD2	2.01922	Hydrogen Bond	Conventional Hydrogen Bond	H-Donor	H-Acceptor
P:POS1:H8 - A:ASP623:OD1	2.08198	Hydrogen Bond	Conventional Hydrogen Bond	H-Donor	H-Acceptor
P:POS1:H10 - A:TYR619:O	2.26365	Hydrogen Bond	Conventional Hydrogen Bond	H-Donor	H-Acceptor
P:POS1:H15 - A:GLU167:OE2	2.34444	Hydrogen Bond	Conventional Hydrogen Bond	H-Donor	H-Acceptor
P:POS1:H17 - A:ASP164:OD1	1.96911	Hydrogen Bond	Conventional Hydrogen Bond	H-Donor	H-Acceptor
P:POS1:H26 - P:POS1:O8	2.43654	Hydrogen Bond	Conventional Hydrogen Bond	H-Donor	H-Acceptor
P:POS1:H26 - P:POS1:O10	2.77541	Hydrogen Bond	Conventional Hydrogen Bond	H-Donor	H-Acceptor
A:ARG553:NH1 - P:POS1	3.12499	Electrostatic	Pi-Cation	Positive	Pi-Orbitals
A:LYS621:NZ - P:POS1	4.73568	Electrostatic	Pi-Cation	Positive	Pi-Orbital
A:ARG624:NH2 - P:POS1	3.72209	Electrostatic	Pi-Cation	Positive	Pi-Orbital
P:POS1 - A:PRO620	4.09681	Hydrophobic	Pi-Alkyl	Pi-Orbitals	Alkyl
P:POS1 - A:VAL166	4.5884	Hydrophobic	Pi-Alkyl	Pi-Orbitals	Alkyl
P:POS1 - A:PRO620	5.27665	Hydrophobic	Pi-Alkyl	Pi-Orbitals	Alkyl

(SASA) is the surface area of a biomolecule (like protein) that is achievable to a solvent. In the current case, the SAS surface showed that 6M71 residues have almost high SAS proclivity (Figure 3c, high SAS/blue color and low SAS/green color). Also, the interpolated charge surface (Figure 3d, blue/red = positive/ negative value), aromatic edge/face surface (Figure 3e, blue/orange = edge/ face), and hydrogen bond donor/acceptor surface (Figure 3f, light violet/ green = donor/ acceptor) have been illustrated base on docking result of 6M71 and RV-18.

In another investigation, the line plot of types of interactions vs. the distance of two centers of interactions has been drawn in

Figure 4I. Conventional hydrogen bond and Pi-alkyl interactions have minimum and maximum distance, respectively, and other forces are between these two points. The energy map visualization dialog is useful to visualize the force fields in MVD (Figure 4II). It seems that to gain an understanding of which regions are attractive to the atoms in a ligand (cobicistat), visualizing these potential fields, such as steric interaction (non-polar atoms) favorable (green color), hydrogen donor favorable (yellow color), hydrogen acceptor favorable (turquoise color), and electrostatic potential of 6M71 (red and blue color) with the RV-12 is necessary and possible.

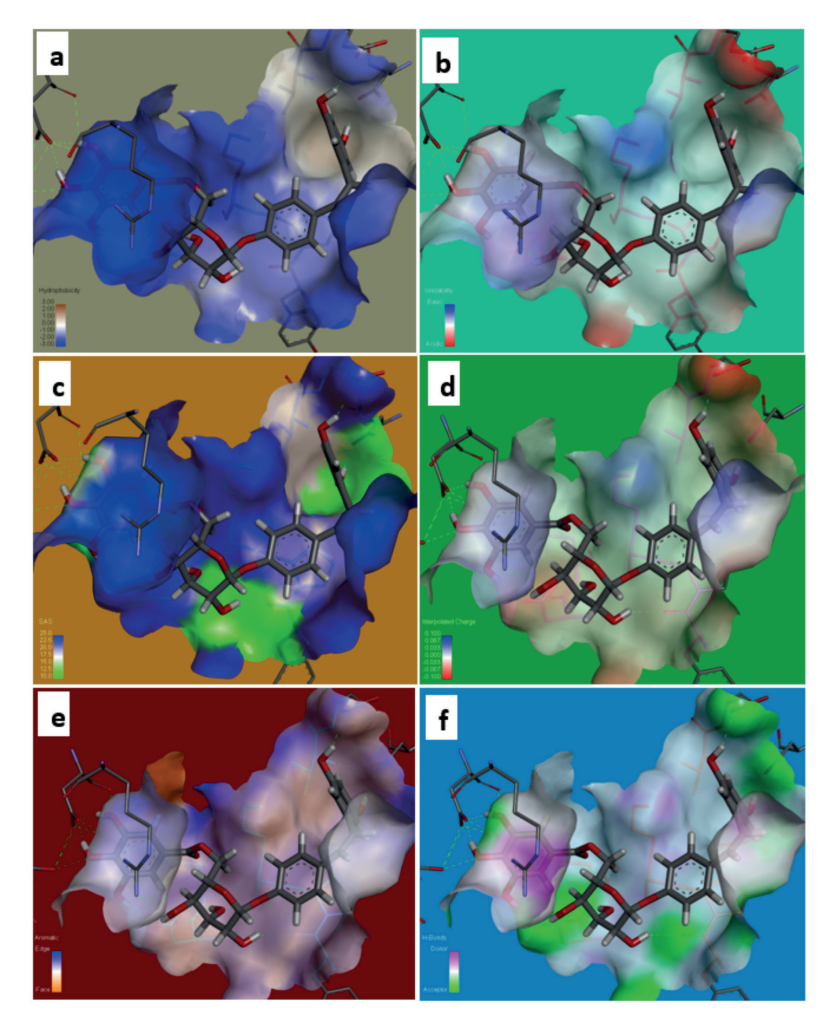


Figure 3. The schematic representation of (a) hydrophobicity (b) ionizability (c) solvent accessibility (d) charge (e) aromatic and (f) H-bond surface of 6M71 around RV-12.

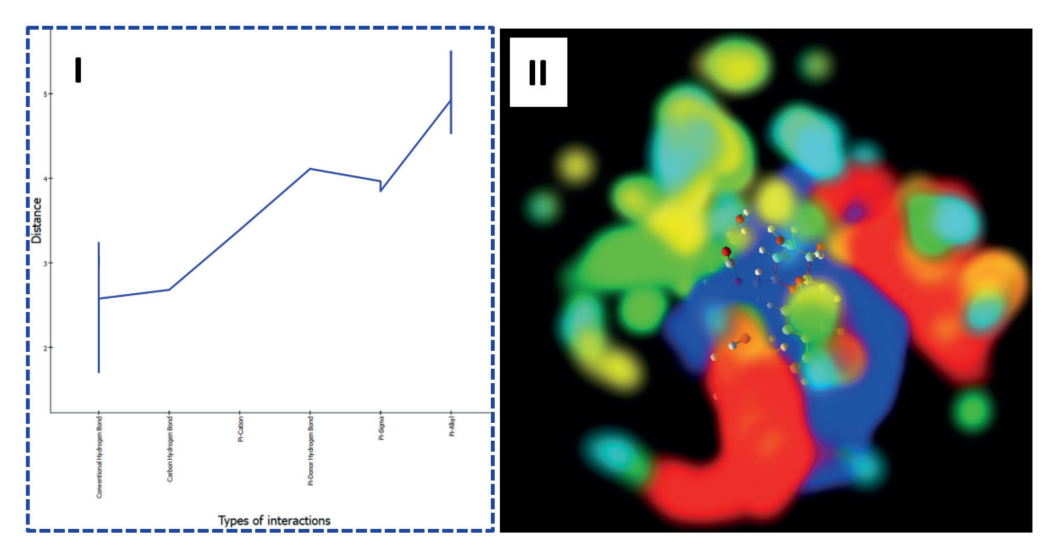


Figure 4. (I) The line plot of types of interactions vs. of distances and (II) Energy map of RV-12 at the binding cavity of 6M71.

7840

Molecular Analysis of Resveratrol Derivatives with 6W9C

Like the previous section, all of the docking analysis was performed by MVD and Discovery Studio 4.5 Client software. As shown in Figure 5, the binding residues of 6W9C have been formed conventional hydrogen bond, Van der Waals, Pi-sigma, and unfavorable doner-doner interactions with RV-13 via the highest MolDock Score. THR 158, ASP 108, THR 158, GLY 160, GLN 269, ASN 109, GLU 161, and THR 158 residues have participated in H-bond formation. The interaction of Pi-orbitals and C-H functional group of LEU 162 residue is introduced Pi-sigma interaction. All these factors and intermolecular forces cause the stability of the desired enzyme and reduce the destructive effect of coronavirus disease (COVID-19). Category, type and distance of interactions have been reported in Table III. The next three ligands that have the most binding energy are as follows: RV-10 (-181.43 kj/mol), RV-11 (-178.10 kj/mol), and RV-12 (-177.56 kj/mol).

Aromatic edge/face, H-bond, charge, solvent accessibility surface (SAS), hydrophobicity, and ionizability receptor surfaces were depicted for the docking result of RV-13 with 6W9C (Figure 6a-f). The plot of types of interactions vs. distances indicated that conventional hydrogen bond interaction is formed in a distance of less than 3.16 angstrom. The maximum distance was observed for Pi-Pi stacked (5.13 angstrom) and Pi-alkyl (5.33 angstrom) interactions. Like the previous section, the plot of types of interactions vs. distanced and the energy map of RV-13 at the binding cavity of 6W9C have been given in Figures 7I and II, respectively.

Conclusions

In this study, molecular modelling techniques have been used to identify and predict the effective targets for the inactivation of COVID-19 receptors. We exported 22 derivatives of the resveratrol compound as a useful medicinal compound from ZINC database.

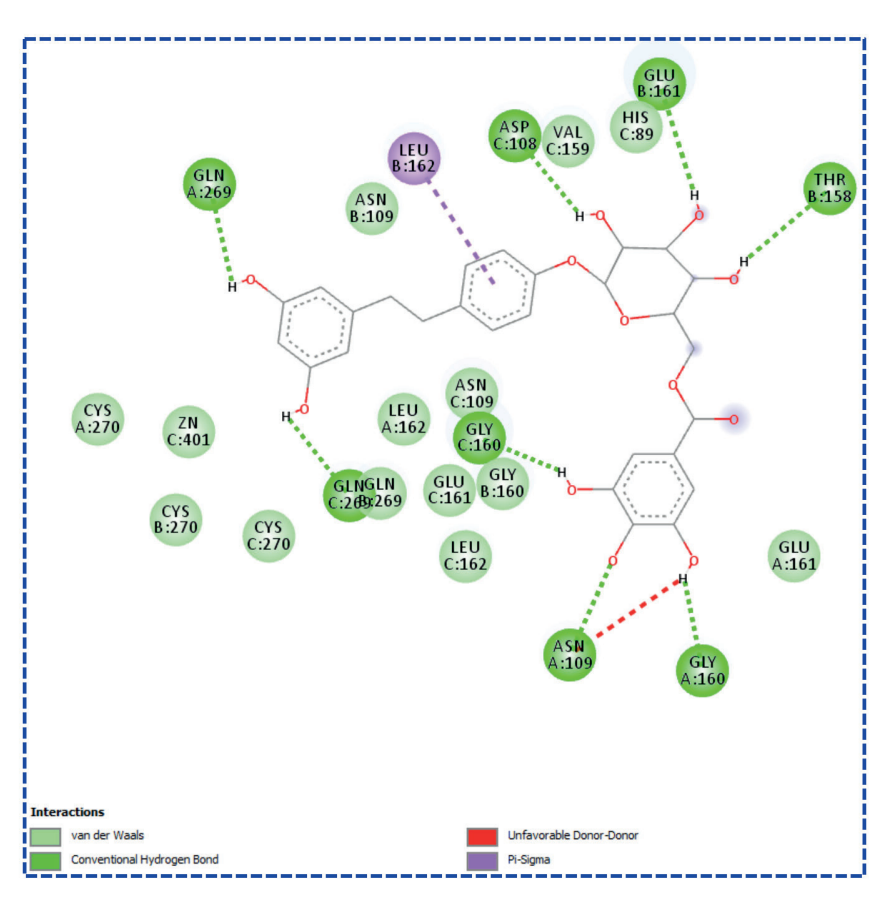


Figure 5. Binding residues and interactions of 6W9C with RV-13.

Table III. The interaction results of RV-12 in binding site of 6M71.

Name	Distance	Category	Туре	From chemistry	To chemistry
A:ASN109:ND2 - P:POS1:O2	3.25445	Hydrogen Bond	Conventional Hydrogen Bond	H-Donor	H-Acceptor
P:POS1:H2 - C:GLY160:O	1.67617	Hydrogen Bond	Conventional Hydrogen Bond	H-Donor	H-Acceptor
P:POS1:H4 - A:GLY160:O	1.90051	Hydrogen Bond	Conventional Hydrogen Bond	H-Donor	H-Acceptor
P:POS1:H6 - B:THR158:OG1	2.33392	Hydrogen Bond	Conventional Hydrogen Bond	H-Donor	H-Acceptor
P:POS1:H8 - B:GLU161:OE1	2.59058	Hydrogen Bond	Conventional Hydrogen Bond	H-Donor	H-Acceptor
P:POS1:H10 - C:ASP108:OD2	2.36675	Hydrogen Bond	Conventional Hydrogen Bond	H-Donor	H-Acceptor
P:POS1:H15 - A:GLN269:O	2.15125	Hydrogen Bond	Conventional Hydrogen Bond	H-Donor	H-Acceptor
P:POS1:H17 - C:GLN269:O	1.7946	Hydrogen Bond	Conventional Hydrogen Bond	H-Donor	H-Acceptor
B:LEU162:CD1 - P:POS1	3.71261	Hydrophobic	Pi-Sigma	С-Н	Pi-Orbitals
P:POS1 - P:POS1	5.09033	Hydrophobic	Pi-Pi Stacked	Pi-Orbitals	Pi-Orbitals
P:POS1 - P:POS1	5.04926	Hydrophobic	Pi-Pi Stacked	Pi-Orbitals	Pi-Orbitals

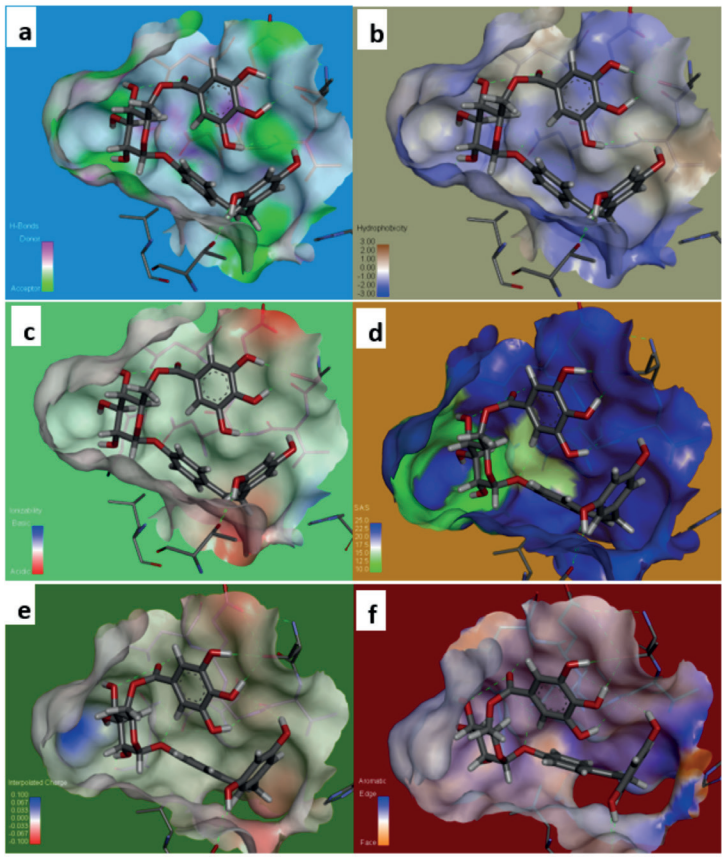


Figure 6. The schematic representation of (a) H-bond (b) hydrophobicity (c) ionizability (d) solvent accessibility (e) charge and (f) aromatic surface of 6W9C around RV-13.

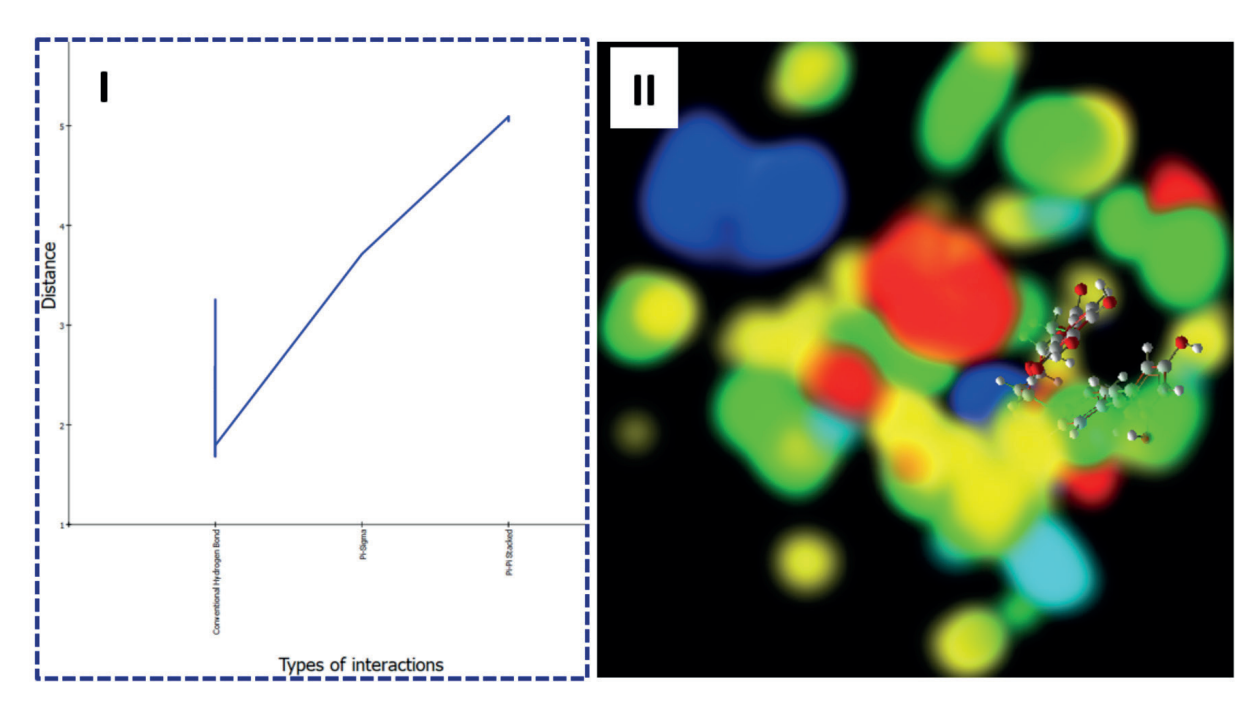


Figure 7. (I) The line plot of types of interactions vs. of distances and (II) Energy map of RV-13 at the binding cavity of 6W9C.

The novel COVID-19 receptors [Papain-like Protease of SARS CoV-2 (PBD ID: 6W9C) and 2019nCoV RNA-dependent RNA Polymerase (PBD ID: 6M71)] were chosen, and the X-ray crystal structures were downloaded from Protein Data Bank database. MVD software was used to calculate and prediction of the binding energy and the binding mode of desired RV derivatives. Also, Discovery Studio 4.5 Client software was applied for the analysis of interactions between the binding residue of enzymes and functional groups of ligands. The result shows that all of the TV derivatives have therapeutic features for COVID-19 outbreak and, RV-12 and RV-13 are the most suitable targets and potential inhibition for 6M71 (173.76 kj/mol) and 6W9C (-184.99 kj/mol), respectively.

Conflict of Interests

The Authors declare that they have no conflict of interests.

References

 JIANG F, DENG L, ZHANG L, CAI Y, CHEUNG CW, XIA Z. Review of the clinical characteristics of coronavirus disease 2019 (COVID-19). J Gen Intern Med 2020; 35: 1545-1549.

- ADEM S, EYUPOGLU V, SARFRAZ I, RASUL A, ALI M. Identification of potent COVID-19 main protease (Mpro) inhibitors from natural polyphenols: An in silico strategy unveils a hope against CORONA. Preprints 2020; 2020030333. Doi: 10.20944/preprints202003.0333.v1.
- CORTEGIANI A, INGOGLIA G, IPPOLITO M, GIARRATANO A, EINAV S. A systematic review on the efficacy and safety of chloroquine for the treatment of COVID-19. J Crit Care 2020; 57: 279-283.
- GAUTRET P, LAGIER JC, PAROLA P, Hydroxychloroquine and azithromycin as a treatment of COVID-19: results of an open-label non-randomized clinical trial. Int J Antimicrob Agents 2020; 105949.
- ARYA R, DAS A, PRASHAR V, KUMAR M. Potential inhibitors against papain-like protease of novel coronavirus (SARS-CoV-2) from FDA approved drugs. ChemRxiv 2020.
- GAO J, TIAN Z, YANG X. Breakthrough: Chloroquine phosphate has shown apparent efficacy in treatment of COVID-19 associated pneumonia in clinical studies. Biosci Trends 2020; 14: 72-73
- Dong L, Hu S, GAO J. Discovering drugs to treat coronavirus disease 2019 (COVID-19). Drug Discov Ther 2020; 14: 58-60.
- ZHAO X, Xu J, Song X, Antiviral effect of resveratrol in ducklings infected with virulent duck enteritis virus. Antivir Res 2016; 130: 93-100.
- 9) CAMPAGNA M, RIVAS C. Antiviral activity of resveratrol. Biochem Soc Trans 2010; 38: 50-53.
- ABBA Y, HASSIM H, HAMZAH H, NOORDIN MM. Antiviral activity of resveratrol against human and animal viruses. Adv Virol 2015; 2015: 184241-184248.

- 11) DWIBEDI V, SAXENA S. *In vitro* anti-oxidant, anti-fungal and anti-staphylococcal activity of resveratrol-producing endophytic Fungi. Proc Natl Acad Sci India Sect B Biol Sci 2020; 90: 207-219.
- FULDA S, DEBATIN K-M. Sensitization for anticancer drug-induced apoptosis by the chemopreventive agent resveratrol. Oncogene 2004; 23: 6702-6711
- MALEKI V, FOROUMANDI E, HAJIZADEH-SHARAFABAD F, KHEIROURI S, ALIZADEH M. The effect of resveratrol on advanced glycation end products in diabetes mellitus: a systematic review. Arch Physiol Biochem 2020; 1-8.
- 14) CHENG CK, Luo JY, LAU CW, CHEN ZY, TIAN XY, HUANG Y. Pharmacological basis and new insights of resveratrol action in the cardiovascular system. Br J Pharmacol 2020; 177: 1258-1277.
- AGUIRRE L, FERNÁNDEZ-QUINTELA A, ARIAS N, PORTILLO MP. Resveratrol: anti-obesity mechanisms of action. Molecules 2014; 19: 18632-18655.
- 16) Koushki M, Lakzaei M, Khodabandehloo H, Hosseini H, Meshkani R, Panahi G. Therapeutic effect of resveratrol supplementation on oxidative stress: a systematic review and meta-analysis of randomised controlled trials. Postgrad Med J 2020; 96: 197-205.
- ROCCARO AM, LELEU X, SACCO A, Resveratrol exerts antiproliferative activity and induces apoptosis in Waldenström's macroglobulinemia. Clin Cancer Res 2008; 14: 1849-1858.
- 18) MA T, TAN M-S, Yu J-T, TAN L. Resveratrol as a therapeutic agent for Alzheimer's disease. BioMed Res Int 2014; 2014: 350516-350529.

- Moretón-Lamas E, Lago-Crespo M, Lage-Yusty M, López-Hernández J. Comparison of methods for analysis of resveratrol in dietary vegetable supplements. Food Chem 2017; 224: 219-223.
- SEBASTIA N, MONTORO A, LEÓN Z, SORIANO JM. Searching trans-resveratrol in fruits and vegetables: a preliminary screening. J Food Sci 2017; 54: 842-845.
- TAUTERMANN CS. Current and future challenges in modern drug discovery. In: Quantum Mechanics in Drug Discovery. Springer, 2020; 2114: 1-17.
- 22) CHANG YC, TUNG YA, LEE KH. Potential therapeutic agents for COVID-19 based on the analysis of protease and RNA polymerase docking, Preprints 2020.
- 23) PAGADALA NS, SYED K, TUSZYNSKI J. Software for molecular docking: a review. Biophys Rev 2017; 9: 91-102.
- MORRIS GM, LIM-WILBY M. Molecular docking. In: Molecular modeling of proteins. Springer 2008; 443: 365-382.
- BITENCOURT-FERREIRA G, DE AZEVEDO WF. Molegro virtual docker for docking. In: Docking Screens for Drug Discovery. Springer 2019; 2053: 149-167.
- Molegro A. MVD 5.0 molegro virtual docker. DK-8000 Aarhus C, Denmark 2011.
- SANDAK B, WOLFSON HJ, NUSSINOV R. Flexible docking allowing induced fit in proteins: insights from an open to closed conformational isomers. Proteins: Structure, Function, and Bioinformatics 1998; 32: 159-174.
- 28) KRIVÁK R, JENDELE L, HOKSZA D. Peptide-Binding site prediction from protein structure via points on the solvent accessible surface. In: Proceedings of the 2018 ACM International Conference on Bioinformatics, Comput Biol Health Inf 2018; 645-650.